



Research Article

Two modified forms of the SAIR model with a fuzzyfied vaccination effectiveness parameter

Harun BALDEMİR^{1,*}, Agah AKIN², Ömer AKIN³

¹Department of Mathematics, Çankırı Karatekin University, Çankırı, 18100, Türkiye

²Dr. Sami Ulus Pediatric Health and Disease Training and Research Hospital, University of Health Sciences, Division of Pediatric Endocrinology, Ankara, 06080, Türkiye

³Department of Mathematics, TOBB Economics and Technology University, Ankara, 06560, Türkiye

ARTICLE INFO

Article history

Received: 27 February 2024

Revised: 05 May 2024

Accepted: 07 June 2024

Keywords:

Asymptomatic Cases;
Compartmental Models;
COVID-19; Fuzzy Modeling;
Vaccination Effectiveness

ABSTRACT

In 2019, the emergence of COVID-19 underscored the critical role of mathematical modeling in understanding and forecasting global health crises. The rapid and often unnoticed spread of infectious diseases by asymptomatic carriers poses a significant challenge to public health efforts worldwide. Understanding and accurately modeling this transmission is crucial for developing effective vaccination strategies and controlling outbreaks. We address this critical issue by enhancing the SAIR model, a Susceptible-Asymptomatic-Infected-Recovered compartmental model, to better capture the dynamics of asymptomatic spread and vaccination effectiveness. This study focuses on the SAIR models to investigate the dynamics of COVID-19 transmission, with a particular emphasis on asymptomatic individuals, who can unknowingly transmit the disease.

In this paper, we present two modifications to the SAIR model. The first modification assumes that individuals gain lifelong immunity after recovering from the infection. The second modification, known as the SAIRS model, considers the possibility of reinfection, meaning recovered individuals can become susceptible again. By applying these enhanced models to real-world data on daily reported COVID-19 cases in Türkiye, we aim to gain a deeper understanding of the pandemic's behavior and progression in the country.

The novelty of this work lies in the integration of a vaccine effectiveness parameter into the SAIR model, uniquely considering the delayed immunity of vaccinated individuals and the distinct transmission dynamics of both symptomatic and asymptomatic cases. Analyzing this parameter within a fuzzy environment enhances the accuracy of predictions, providing more dependable estimations of future disease scenarios. This approach offers a new dimension to epidemic modeling, contributing valuable insights to public health strategies and vaccination policies.

Cite this article as: Baldemir H, Akın A, Akın Ö. Two modified forms of the SAIR model with a fuzzyfied vaccination effectiveness parameter. Sigma J Eng Nat Sci 2025;43(3):887–898.

*Corresponding author.

*E-mail address: harunbaldemir@karatekin.edu.tr

This paper was recommended for publication in revised form by
Editor-in-Chief Ahmet Selim Dalkilic



INTRODUCTION

Coronaviruses are a diverse family of viruses known to infect both animals and humans, causing a wide spectrum of illnesses. These illnesses range from mild respiratory conditions, such as the common cold, to more severe diseases like Middle East Respiratory Syndrome (MERS) and Severe Acute Respiratory Syndrome (SARS) in humans [1, 2]. In 2019, a novel coronavirus, named severe acute respiratory syndrome coronavirus 2 (SARS-CoV-2), was identified as the root cause of a significant outbreak of pneumonia cases in China. This new virus rapidly spread, initially causing an epidemic within China, and swiftly expanding its global reach [3-5]. Recognizing the scale of the crisis, the World Health Organization promptly declared it a global pandemic, officially designating the disease as COVID-19, denoting the coronavirus disease of 2019 [6].

Mathematical modelling plays a pivotal role in the study of epidemics, serving not only to unravel the progression of diseases but also to offer forecasts regarding their future evolution [7–10]. The use of mathematical modeling approaches to understand the spread of epidemics has a long history. However, beginning in the middle of the 20th century, mathematical epidemiology appears to have expanded tremendously. Hethcote [11] provided a detailed review of the mathematical modeling of infectious diseases, offering a comprehensive exploration of methodologies and techniques. Furthermore, mathematical modelling provides valuable insights into the dynamics, patterns and behaviours of epidemics, particularly in the context of a fuzzy environment [12-14].

Epidemiological models divide people into sub-groups or compartments such as healthy individuals but susceptible to the infection (*Susceptible (S)*), individuals currently carrying the infection (*Infected (I)*), recovered people from the disease (*Recovered (R)*). The disease is transmitted from the individuals in the infected compartment to the people in the susceptible compartment. This type of models are called *SIR (Susceptible-Infected-Recovered) type models* or, more broadly, as *compartmental models*. Research on epidemic modeling, particularly in the context of COVID-19, has been pivotal in understanding and predicting disease dynamics. Numerous studies have applied to SIR type models to analyze real-time data, providing valuable insights into the spread, transmission patterns, and impact of the virus [14-16].

The SIR model is defined by a system of three coupled non-linear ordinary differential equations [17]. Adding new compartments or new parameters can extend the model [18-20]. For example, in the SEIR model *E* stands for the group that have been infected but is not yet infectious, in the SIRD model, *D* stands for the group of deaths due to the disease, and in the SAIR model, *A* stands for the group of asymptomatic individuals that do not show any symptoms of the disease but spread the disease to others.

Government officials and public health decision-makers recognize the critical importance of isolating symptomatic

individuals from healthy ones to protect the broader population from the rapid transmission of diseases [21, 22]. Nonetheless, the presence of unreported subclinical cases presents a significant challenge when attempting to accurately determine the rate of disease transmission [23-25]. Therefore, it is crucial to investigate the influence of asymptomatic individuals on the spread of disease.

MODIFICATIONS ON THE SAIR MODEL

In this joint paper, we present modifications to the SAIR model originally introduced by Robinson and Stilianakis in 2013 [26]. The SAIR model classifies the population into four distinct sub-groups or compartments, specifically as susceptible (*S*), asymptomatic (*A*), infected (*I*), and recovered (*R*). Notably, the infected individuals are further categorized into two compartments. The first group, referred to as “asymptomatic (*A*),” comprises individuals who remain free of disease symptoms but can still transmit the infection. The second group, named “infected (*I*),” includes individuals displaying symptoms of the disease.

The transitions among subgroups in the modified SAIR models are visually represented in a schematic illustration in Figure 1. Individuals in the susceptible (*S*) group become infected upon contact with either symptomatic or asymptomatic infected individuals. Following contraction of the disease, they initially transition to the asymptomatic state, often with a delay between infection and the onset of symptoms. Subsequently, if symptoms develop, individuals progress to the symptomatic state of infection, namely the infected (*I*) group. Alternatively, they may move directly to the recovered (*R*) group without developing any symptoms. The left panel of Figure 1 illustrates the scenario of lifelong immunity, while the right panel depicts the possibility of non-lifelong immunity in the SAIRS model.

In our models, we have streamlined the model originally proposed by Robinson and Stilianakis [26], omitting constant birth and natural death rates for simplification. Instead, we introduce a crucial parameter to account for vaccination effectiveness. For example, the vaccine was added to the SAIR model in [20], but individuals were directly transferred into the recovered group. Our proposed approach differs by addressing the specific scenario where vaccinated individuals do not immediately enter the recovered state, which introduces a novel dimension to the analysis of disease spread in the presence of vaccination. To the best of our knowledge, this paper stands as the first integration of the vaccination effectiveness parameter into the SAIR model, while considering that vaccinated individuals do not directly transition to the recovered compartment.

Understanding the impact of vaccination is crucial for managing pandemics like COVID-19. With this adaptation, our objective is to gain a more comprehensive understanding of how vaccinations impact disease dynamics and transmission. This refined approach allows for a focused exploration of the complex interaction between vaccination

efficacy and the spread of the disease, potentially revealing invaluable insights to guide and improve public health strategies and vaccination campaigns.

One of the two altered SAIR models is referred to as *the modified SAIR model with lifelong immunity* as visually illustrated in the left panel of Figure 1. Here we assume that all infected individuals eventually return to a healthy state. The system of the model is given below;

$$\begin{aligned} \frac{dS}{dt} &= -[\tau\beta_A A + (1 - \tau)\beta_I I]S \\ \frac{dA}{dt} &= [\tau\beta_A A + (1 - \tau)\beta_I I]S - \delta A - \gamma_A A \\ \frac{dI}{dt} &= \delta A - \gamma_I I \\ \frac{dR}{dt} &= \gamma_A A + \gamma_I I. \end{aligned}$$

Here, β_A and β_I are the transition rates of the asymptomatic and symptomatic compartments respectively, γ_A and γ_I are the recovery rate from the asymptomatic and symptomatic infections respectively, δ is the rate of pre-clinical individuals from the asymptomatic to the symptomatic compartment; and τ is the vaccine effectiveness parameter.

Introducing our second modified model, known as *the modified SAIR model with non-lifelong immunity (or the modified SAIRS model)*, we introduce a new parameter denoted as α . This parameter signifies the transition from compartment R to compartment S as seen in the right panel of Figure 1. In this model, we assume that immunity following recovery is of a temporary nature. As a result, individuals who have recovered lose their immunity and return to a susceptible state. The system of this model is as follows:

$$\begin{aligned} \frac{dS}{dt} &= -[\tau\beta_A A + (1 - \tau)\beta_I I]S + \alpha R \\ \frac{dA}{dt} &= [\tau\beta_A A + (1 - \tau)\beta_I I]S - \delta A - \gamma_A A \\ \frac{dI}{dt} &= \delta A - \gamma_I I \\ \frac{dR}{dt} &= \gamma_A A + \gamma_I I - \alpha R \end{aligned}$$

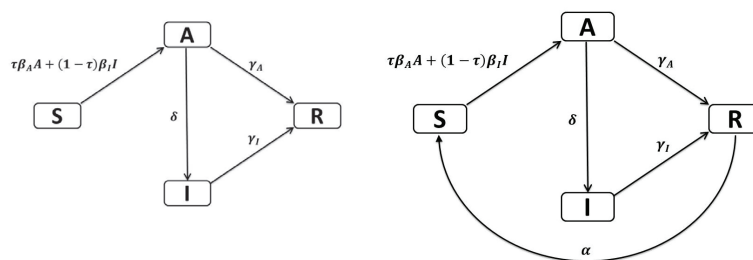


Figure 1. The flow diagrams of SAIR models with lifelong (left panel) and non-lifelong (right panel) immunity.

In both of the modified SAIR models, we consider a normalized population, i.e.

$$S_t + A_t + I_t + R_t = 1.$$

where P_t denotes the number of individuals in the compartment P at time t . This normalization allows us to focus on relative proportions and analyze disease dynamics within a consistent and closed population.

In our study, we estimate the transition parameters among compartments by fitting the real data in a least squares sense. This process involves finding optimal parameters for our models by minimizing the difference between the observed data and model predictions. It is a common practice in various scientific fields, allowing for accurate analysis and prediction using real-world data.

We obtain our real-world data from daily reports provided by the Ministry of Health of Turkey [27]. Along with fitting the model to the real data, we also consider future disease estimations for various time periods to assess the performance of the models over time.

Recognizing that epidemiological research often involves inherent imprecision and uncertainty, particularly given the diverse ways diseases can manifest, we incorporate fuzzy logic into our methodology. This approach enhances the precision and accuracy of our results, particularly in situations where imprecision and uncertainty are common.

Fuzzy Modelling

Fuzzy modeling, originating from the pioneering work of Lotfi A. Zadeh, who introduced the fuzzy set theory [28], has evolved into a fundamental tool for addressing the vagueness and uncertainty frequently associated with scientific concepts. These notions of imprecision and uncertainty play a pivotal role in various scientific and real-world scenarios. In the pursuit of more accurate mathematical representations, Zadeh pioneered a new set concept, one that extended beyond the traditional boundaries of crisp set theory, incorporating elements with a function known as the membership function, denoted as $\mu(X) = X \rightarrow [0,1]$, with X representing the universal set in a given context.

Fuzzy logic, derived from the fuzzy set theory, notably emphasizes the concept of degrees of belonging [29,

30]. This refined approach deviates from rigid categorizations of right or wrong, instead focusing on the shades of gray that exist in between. Over the years, fuzzy logic has evolved significantly, emerging as a powerful tool for effectively modeling and addressing uncertainty, a feature particularly valuable in fields such as artificial intelligence, decision-making systems, and control engineering [31, 32].

The search of precision and efficiency has driven the exploration of various methods that utilize fuzzy logic to offer optimal solutions in practical scenarios [33, 34]. Fuzzy modeling has found its application in diverse domains, from classifying vegetation units in ecological studies to interpreting and refining weather forecasts, thus exemplifying its enduring relevance in addressing multifaceted aspects of life today [35, 36].

The integration of fuzzy logic in SIR type models has been explored in recent research, showcasing its potential to enhance the adaptability and precision of these models. For instance, [14] investigated an SIR epidemic model for COVID-19 spread with fuzzy parameters, emphasizing the importance of incorporating uncertain parameters to reflect real-world complexities. These studies underscore the growing significance of fuzzy parameters in SIR-type models, offering valuable insights into the complexities of infectious disease dynamics and their control. The adaptability and the concept of degrees of membership make fuzzy modeling an invaluable tool for handling real-world scenarios characterized by uncertainty and imprecision, ultimately enhancing the decision-making and problem-solving capabilities across a spectrum of disciplines [37, 38].

Contributions and Organization of the Paper

Firstly, we employ modified SAIR models as a primary tool. These models enable us to derive valuable insights into the complex patterns of disease transmission, the effectiveness of control measures, and the influence of vaccination strategies. By adapting these models to the unique circumstances of the pandemic, we aim to provide a deeper understanding of the COVID-19 dynamics within Turkey.

Our focus centers on analyzing the dynamics of COVID-19 through the examination of real-time data on daily reported cases in Turkey, provided by the Ministry of Health. In a significant and innovative step, we extend the classical SAIR models into a fuzzified environment by expanding the traditional, crisp vaccination parameter τ into a fuzzy set theoretical framework. This extension is crucial, as it provides us with the ability to account for the various uncertainties and vagueness that often surround vaccination strategies.

Our proposed approach introduces a novel dimension to the analysis of disease spread in the presence of vaccination by addressing the specific scenario where vaccinated individuals do not immediately transition to the recovered state. To the best of our knowledge, this paper represents the pioneering instance of incorporating the vaccination

effectiveness parameter into the SAIR model under these considerations, offering a unique and valuable perspective on disease dynamics. Additionally, the incorporation of a fuzzy logic framework enhances the practicality and applicability of our findings. Our aspiration is that these research outcomes will be instrumental in guiding policymakers and health authorities as they formulate and fine-tune more effective strategies to combat the disease. This paper thus contributes to the advancement of disease modeling and provides valuable insights that may play a crucial role in reducing the impact of the virus.

The organization of this paper follows a structured framework. Introduction section sets the stage for our comprehensive analysis. Within this section, we provide essential background information, covering topics such as coronaviruses, mathematical modeling, and SIR-type models. Furthermore, we discuss the modifications of the SAIR Model, considering both lifelong and non-lifelong immunity, and clarify the concept of fuzzy modeling, emphasizing its significance in addressing vagueness and uncertainty. Additionally, we examine the vaccine effectiveness parameter, considering its impact on disease transmission in a fuzzy context.

In the result section, we focus on two specific time periods characterized by rapid increases in daily active COVID-19 cases. We examine the parameter estimations of both modified SAIR models, one with lifelong immunity and the other with non-lifelong immunity. Additionally, our study includes a forward-looking analysis of 7 days taking into account the vaccine effectiveness parameter within a fuzzy environment for both time periods using these models.

Finally, we provide a summary of the paper and discuss the key findings and results in the conclusion section.

The derived knowledge from the literature review highlights the critical importance of understanding the dynamics of infectious diseases, particularly concerning asymptomatic transmission and vaccination effectiveness. Synthesizing insights from previous studies, we identified gaps in current modeling approaches, specifically the need to incorporate lifelong immunity and the possibility of reinfection into existing models. Additionally, our review underlines the significance of considering delayed immunity in vaccination strategies to provide a more accurate representation of disease transmission dynamics. The novelty of this work lies in the innovative modifications to the traditional SAIR model to incorporate both lifelong immunity and the possibility of reinfection, resulting in the SAIRS model. Moreover, our integration of a vaccine effectiveness parameter that accounts for delayed immunity provides a more realistic representation of vaccination impacts on disease transmission. By applying these enhanced models to real-world data from COVID-19 cases in Turkey and analyzing them within a fuzzy environment, we can achieve more accurate and reliable predictions of future disease scenarios.

RESULTS AND DISCUSSION

Epidemics of viruses have consistently presented major health problems, leading to high mortality rates in human communities. This joint article focuses on understanding the outbreak of the coronavirus in Turkey, employing essential mathematical models to analyze its spread and impact on public health and the healthcare system. Mathematical models play a crucial role in systematically quantifying disease transmission dynamics, considering various factors such as assumptions, variables, and parameters. Researchers continuously validate and fine-tune these models by comparing their predictions with real-world data, aiding in effective public health responses and guiding strategies for future challenges.

In this section, we apply the modified SAIR models with lifelong and non-lifelong immunity to the real data (the number of infected and recovered cases) of COVID-19 in Turkey in order to estimate the parameters in the models.

In Figure 2, we show the numbers of the daily active cases in the upper panel and the cumulative recovered cases in lower panel, where the data is obtained from the Ministry of Health of Turkey. It is important to emphasize that the daily active cases differ from the daily new cases reported by the Ministry of Health at the end of each day. The daily active cases are computed by subtracting the total of recovered and deceased cases from the overall infected cases, as expressed in the formula:

$$\text{Active cases} = \text{Infected cases} - (\text{Recovered cases} + \text{Deaths}).$$

It is seen from the upper panel of Figure 2 that there are several peaks in the number of the daily active cases. We focus on two periods (shaded regions P_1 and P_2) where

rapid increases in the number of the daily active cases occurred. Here; P_1 denotes the period from 13 March to 20 April 2021 and P_2 denotes the period from 23 December 2021 to 10 January 2022. In both time intervals, we apply the real data to our models, resulting in the estimation of the model parameters for each period.

The Modified SAIR Model with Lifelong Immunity

We should consider that the modified SAIR models given in systems (1) and (2) are normalized models. Therefore, to estimate the model parameters effectively, the real data needs to be prepared for fitting the normalized model in each period.

Data preparation involves several steps. Firstly, we normalize the data, which includes the counts of infected, recovered, and deaths. This normalization process entails dividing each data set by the maximum value of the recovered cases, ensuring that all values fall within the range of 0 to 1.

Data preparation is a critical phase in our analysis, involving several essential steps. Firstly, we initiate the process by normalizing the data, specifically focusing on infected, recovered, and deaths. This normalization procedure involves dividing each dataset by the maximum value of the recovered cases, ensuring that all data points are scaled to fall within the standardized range of 0 to 1.

Additionally, it is crucial to emphasize that we treat each period as an independent entity. In other words, at the beginning of each period, there are initially some individuals with infections ($I_0 > 0$) and no individuals in the recovered state ($R_0 = 0$). This separation of periods is a fundamental aspect of our modeling approach, allowing us to customize our analysis to the unique characteristics and dynamics of each time segment.

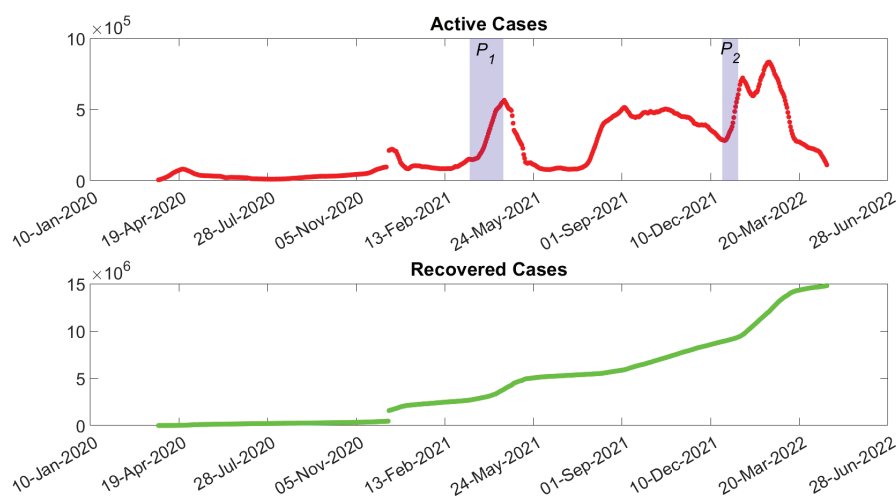
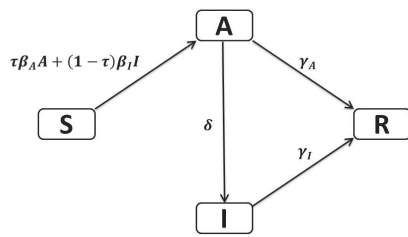


Figure 2. Daily number of active cases (upper panel) and cumulative number of recovered cases (lower panel) of COVID-19 in Turkey. Two distinct periods are indicated by shaded regions P_1 and P_2 where the number of daily active cases show rapid increases. In the upper panel, P_1 denotes the period from 13 March to 20 April 2021, and P_2 denotes the period from 23 December 2021 to 10 January 2022.



$$\begin{aligned} \frac{dS}{dt} &= -[\tau\beta_A A + (1-\tau)\beta_I I]S \\ \frac{dA}{dt} &= [\tau\beta_A A + (1-\tau)\beta_I I]S - \delta A - \gamma_A A \\ \frac{dI}{dt} &= \delta A - \gamma_I I \\ \frac{dR}{dt} &= \gamma_A A + \gamma_I I. \end{aligned}$$

Figure 3. The flow diagram and the model equations of the modified SAIR Model with lifelong immunity.

We now have the data appropriately normalized for active and recovered cases. The number of active cases will be used to fit the data with the infected (*I*) compartment and the number of recovered cases will be employed to model the recovered compartment (*R*). Additionally, we also need the initial values for the susceptible (*S*) and asymptomatic (*A*) compartments. Given that the number of asymptomatic individuals tends to be notably higher than symptomatic individuals, we assume that the initial count of asymptomatic individuals is double that of symptomatic individuals (i.e., $A_0 = 2I_0$). Finally we can calculate the initial value of susceptible (*S*) compartment as $S_0 = 1 - A_0 - I_0 - R_0$ since the sum of the normalized constant population is given by $S_t + A_t + I_t + R_t = 1$.

The modified SAIR model with lifelong immunity shown in Figure 3 has six parameters; namely the transition rate of the asymptomatic compartment β_A , the transition rate of the symptomatic compartment β_I , the recovery rate from the asymptomatic infection γ_A , the recovery rate from the

symptomatic infection γ_I , the rate of pre-clinical individuals from the asymptomatic to the symptomatic state δ and the vaccine effectiveness parameter τ . Using the built-in function *lsqcurvefit* in MATLAB software [39], we estimate these parameters using the real data of the active and recovered cases during the period P_1 and show the estimations of the model parameters in Table 1. We note that the value of β_A is greater than the value of β_I as expected since the transition of the virus is largely carried by asymptomatic individuals. This observation aligns with findings from previous research emphasizing the substantial role of asymptomatic carriers in disease transmission dynamics [21, 23]. The higher estimated transition rate of the asymptomatic compartment (β_A) underscores the importance of considering the contribution of asymptomatic individuals when modeling disease spread. Estimating these parameters is crucial as they provide valuable insights into the underlying mechanisms driving COVID-19 transmission dynamics, aiding in more informed decision-making by public health authorities.

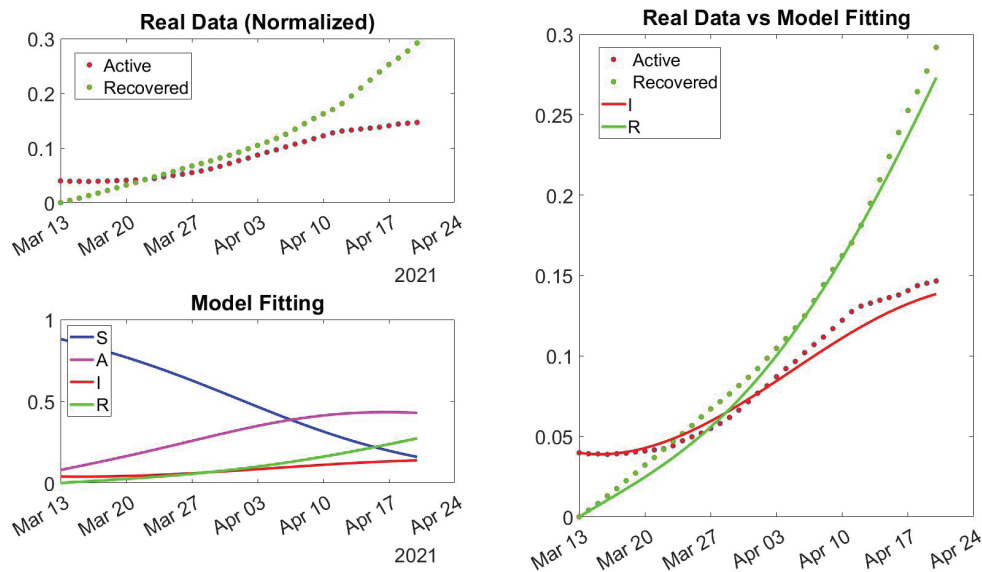


Figure 4. Application of the modified SAIR model with lifelong immunity to the real data for the period P_1 . The upper left figure shows the normalized data of daily number of active cases and cumulative number of recovered cases during the period P_1 from 13 March to 20 April 2021. The lower left figure illustrates model simulation. The right figure provides a visual comparison of the real data (filled circles) and the model fitting (solid curves).

Table 1. Parameter estimation of the modified SAIR model with lifelong immunity using the real data of active and recovered cases during the period P_1 from 13 March to 20 April 2021

Model parameters	β_A	β_I	γ_A	γ_I	δ	τ
Estimated values	0.3653	0.3243	0.0001	0.0882	0.0324	0.2179

In Figure 4, we show the model fitting to the real data for the period P_1 from 13 March to 20 April 2021. The upper left panel of Figure 4 shows the real data of the active (filled red circles) and recovered cases (filled green circles) normalized by the maximum of the recovered cases in the period P_1 (from 13 March to 20 April 2021). The lower left panel shows the model simulation using the parameters estimated by the real data. Here, the solid blue curve represents the susceptible (S) compartment, the solid purple curve represents the asymptomatic (A) compartment, the solid red curve represents the infected (I) compartment, and the solid green curve represents the recovered (R) compartment. It is seen that the asymptomatic (A) curve (purple) is located above the the symptomatic (I) curve (red). This observation aligns with the fact that asymptomatic individuals, often more numerous in society, play a significant role in disease transmission. The right panel of Figure 4 shows the comparison between the normalized real data and the model simulation. The model demonstrates a strong alignment with both active and recovered cases. For comprehensive parameter values related to this period, refer to Table 1.

Fitting the model to the real data of the second period (P_2), we can extract the estimated model parameters tailored to the unique characteristics of P_2 . The estimated model parameters for the two periods are given in Table 2.

Now that we have successfully estimated the parameters for both periods, we can illustrate the model's performance by comparing it with the real data over an extended time-frame. This extended analysis allows us to assess how well the model aligns with the actual data beyond the initial periods of study.

In Figure 5a, we extend our analysis for an additional 7 days, commencing on 20 April 2021, immediately following the conclusion of period P_1 . During this 7-day extension, we continue to track the performance of the model, and it is evident that we achieve a strong alignment between the model (illustrated by solid lines) and the real data (illustrated by data points). This observation emphasizes the model's effectiveness in capturing and predicting the dynamics of the COVID-19 outbreak.

A similar analysis was conducted for period P_2 , as depicted in Figure 5b. Here, we examined the performance

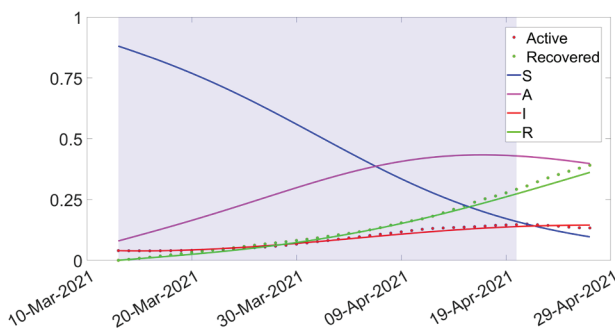


Figure 5a. 7 days of future estimation for the period P_1 . The shaded region illustrates the model fitting to real data for the period P_1 from 13 March to 20 April 2021. The white region represents the comparison between the model estimation and the real data for an additional 7 days until 27 April 2021.

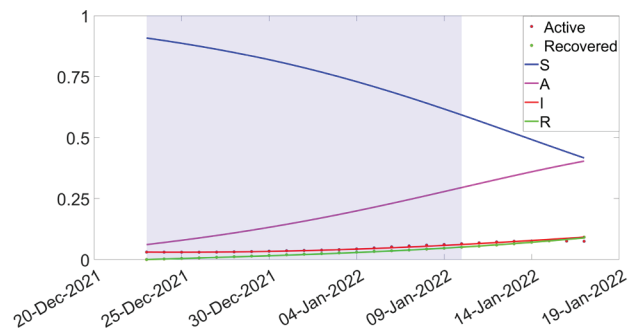


Figure 5b. 7 days of future estimation for the period P_2 . The shaded region illustrates the model fitting to real data for the period P_1 from 23 December 2021 to 10 January 2022. The white region represents the comparison between the model estimation and the real data for an additional 7 days until 17 January 2022.

Figure 5. 7 days of future estimation of the SAIR model with lifelong immunity for periods and

Table 2. Parameter estimation of the modified SAIR model with lifelong immunity using the real data of active and recovered cases during the periods P_1 from 13 March to 20 April 2021 and P_2 from 23 December 2021 to 10 January 2022

	β_A	β_I	γ_A	γ_I	δ	τ
P_1	0.3653	0.3243	0.0001	0.0882	0.0324	0.2179
P_2	0.3526	0.2268	0.0001	0.0712	0.0277	0.3110

of the model for an additional 7 days, starting from 10 January 2022. Once again, we found a compelling fit between the model and the real data, confirming the model’s reliability in projecting short-term trends and outcomes beyond the initial study periods.

In our pursuit of a more comprehensive understanding of the dynamics of COVID-19 and the efficacy of vaccination in Turkey, we have taken a step further by transforming the modified SAIR model with lifelong immunity into a fuzzified environment. This transition introduces a degree of fuzziness into the model, providing us with a more flexible framework that can better account for the complexities and uncertainties associated with the real-world data.

The crisp vaccination parameter τ holds a central role in our model. It represents the effectiveness of vaccination efforts in reducing disease transmission. The value of τ directly influences how the model simulates the interplay between vaccinated and unvaccinated individuals in a population, affecting the overall disease dynamics. By extending this parameter into a fuzzy sense, we acknowledge that the real-world effectiveness of vaccination is not a fixed, precise value. Instead, it can vary in response to numerous factors such as vaccine coverage, vaccine hesitancy, and the emergence of new variants.

As displayed in Table 2, we have calculated crisp values for the vaccination parameter τ for two distinct periods, with values of 0.2179 for P_1 and 0.3110 for P_2 . However, upon closer examination of the crisp solutions in Figure 6, we notice that some segments of these solutions deviate either above or below the real data points. This deviation suggests that the model’s performance could be further enhanced by exploring a range of values for the vaccination parameter τ during these specific periods, thus introducing a sense of fuzziness. By investigating these upper and

lower bounds for the vaccination parameter τ , we aim to gain deeper insights into the vaccine’s real-world impact on disease dynamics. This approach not only makes our model more adaptable to the variable nature of COVID-19 but also better aligns it with the complexities of the fluctuations and dynamics of the pandemic.

In Figure 6, we explore the lowest and the highest bounds of the α -cuts for the parameter τ for P_1 , which range from 0.1179 to 0.3179. In the fuzzy environment, we can express this as $[0.2179]^\alpha = [0.1179 + 0.1\alpha, 0.3179 - 0.1\alpha]$ where $0 \leq \alpha \leq 1$. Similarly, we examine the lowest and the highest bounds of the α -cuts for the parameter τ for P_2 , which span from 0.2110 to 0.4110. In fuzzy theory, we can state this as $[0.3110]^\alpha = [0.2110 + 0.1\alpha, 0.4110 - 0.1\alpha]$ where $0 \leq \alpha \leq 1$. As a result, we observe that the real data points for both P_1 and P_2 fall within the curves defined by these upper and lower bounds. This observation highlights the dynamic nature of the fuzzy framework in addressing the variability and uncertainties associated with the real data. Consequently, it provides a more robust representation of the complex dynamics of the COVID-19 pandemic during these periods.

The Modified SAIR Model with Non-Lifelong Immunity

In this section, we replicate the computations performed for the modified SAIR model with lifelong immunity in the context of the modified SAIR model with non-lifelong immunity as shown in Figure 7.

We estimate the model parameters using real data on active and recovered cases during periods P_1 and P_2 , presenting the parameter estimations in Table 3. It’s worth noting that, as expected for SAIR models, the value of β_A is greater than that of β_I .

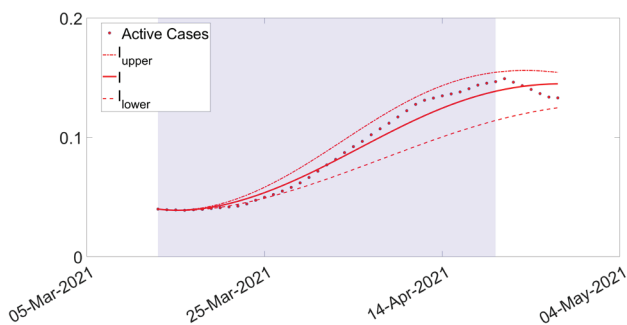


Figure 6a. Fuzzy environment for the period P_1 with a 7-day future estimation. I , I_{upper} , and I_{lower} represent the crisp, upper-bound, and lower-bound solutions, respectively. The shaded region illustrates the model fitting to real data for the period P_1 from March 13 to April 20, 2021. The white region represents the comparison between the model estimation and real data for an additional 7 days until 27 April 2021.

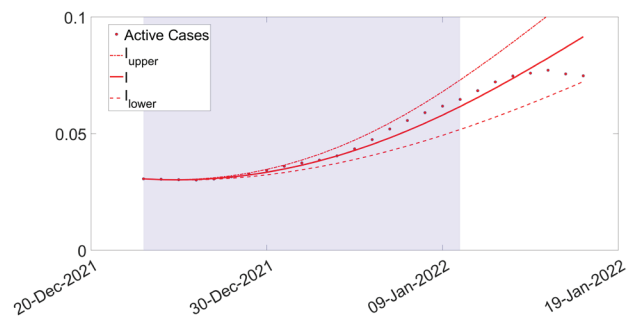


Figure 6b. Fuzzy environment for the period P_2 with a 7-day future estimation. I , I_{upper} , and I_{lower} represent the crisp, upper-bound, and lower-bound solutions, respectively. The shaded region illustrates the model fitting to real data for the period P_2 from 23 December 2021 to 10 January 2022. The white region represents the comparison between the model estimation and real data for an additional 7 days until 17 January 2022.

Figure 6. Simulation of the modified SAIR model with lifelong immunity using the vaccine effectiveness parameter τ in fuzzy environment for the periods P_1 and P_2 .

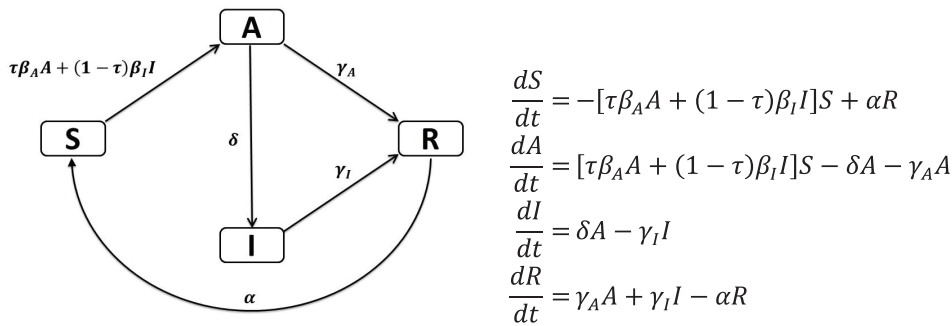


Figure 7. The flow diagram and the model equations of the modified SAIR Model with non-lifelong immunity.

Table 3. Parameter estimation of the modified SAIR model with non-lifelong immunity using the real data of active and recovered cases during the periods P_1 from 13 March to 20 April 2021 and P_2 from 23 December 2021 to 10 January 2022

	β_A	β_I	γ_A	γ_I	δ	τ	α
P_1	0.3823	0.0001	0.0001	0.0981	0.0354	0.3926	0.0074
P_2	0.5072	0.3030	0.0167	0.0536	0.0192	0.2661	0.1296

With the estimated parameters now available for both periods P_1 and P_2 , we can proceed to compare the model’s performance with real data over an extended time frame. In Figure 8a, we continue our analysis for an additional 7 days, commencing on April 20, 2021, immediately following the conclusion of the period P_1 . This extension reveals a close alignment between the predictions of the model (solid lines) and the real data (data points).

We have similarly executed a parallel analysis for the period P_2 , as illustrated in Figure 8b, encompassing an additional 7 days starting from January 10, 2022. This extended analysis confirms the ability of the model to offer accurate predictions and highlights its effectiveness in capturing the

dynamics of the COVID-19 outbreak, even beyond the initially studied periods.

We now adapt the modified SAIR model with non-lifelong immunity to a fuzzy environment, extending the crisp vaccination parameter τ in a fuzzy context. As indicated in Table 3, the crisp values of the vaccination parameter τ are 0.3926 and 0.2661 for periods P_1 and P_2 , respectively. In Figure 6, some parts of the crisp solutions for both periods P_1 and P_2 exhibit values that are either above or below the real data. Consequently, we proceed to explore a range for the upper and lower bounds of the vaccination parameter τ for these specific time intervals.

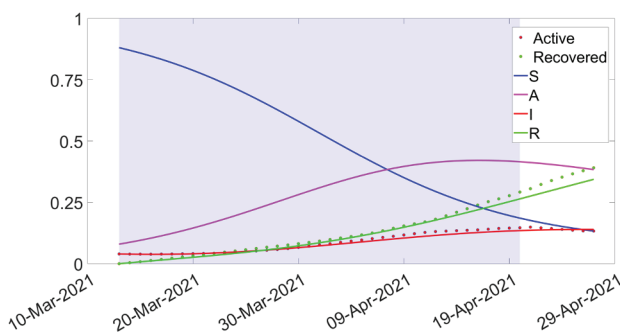


Figure 8a. 7 days of future estimation for the period P_1 . The shaded region illustrates the model fitting to real data for the period P_1 from 13 March to 20 April 2021. The white region represents the comparison between the model estimation and the real data for an additional 7 days until 27 April 2021.

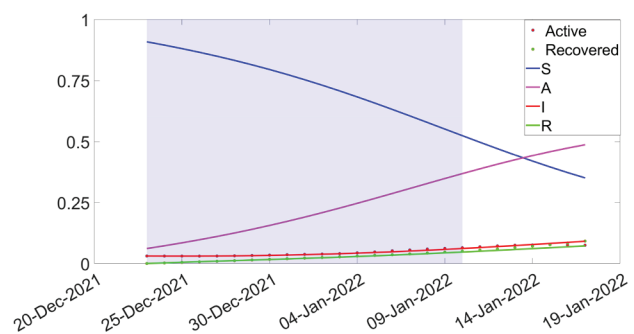


Figure 8b. 7 days of future estimation for the period P_2 . The shaded region illustrates the model fitting to real data for the period P_1 from 23 December 2021 to 10 January 2022. The white region represents the comparison between the model estimation and the real data for an additional 7 days until 17 January 2022.

Figure 8. 7 days of future estimation of the SAIR model with non-lifelong immunity for period and

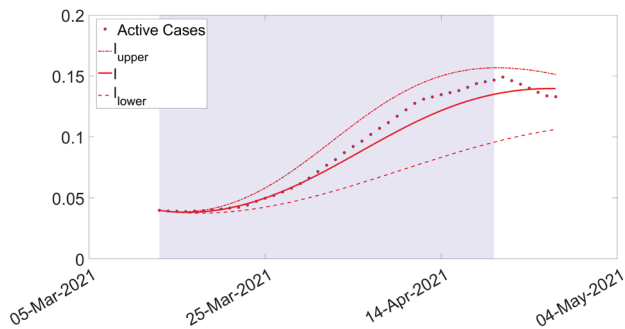


Figure 9a. Fuzzy environment for the period P_1 with a 7-day future estimation. I , I_{upper} , and I_{lower} represent the crisp, upper-bound, and lower-bound solutions, respectively. The shaded region illustrates the model fitting to real data for the period P_1 from March 13 to April 20, 2021. The white region represents the comparison between the model estimation and real data for an additional 7 days until 27 April 2021.

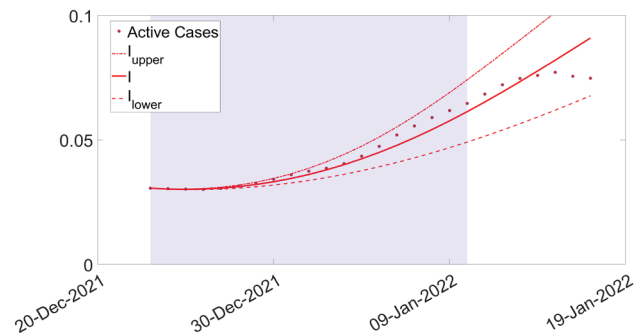


Figure 9b. Fuzzy environment for the period P_2 with a 7-day future estimation. I , I_{upper} , and I_{lower} represent the crisp, upper-bound, and lower-bound solutions, respectively. The shaded region illustrates the model fitting to real data for the period P_2 from 23 December 2021 to 10 January 2022. The white region represents the comparison between the model estimation and real data for an additional 7 days until 17 January 2022.

Figure 9. Simulation of the modified SAIR model with non-lifelong immunity using the vaccine effectiveness parameter in fuzzy environment for the periods and

In Figure 9, we establish the lower and upper bounds of the α -cuts for the parameter τ within P_1 , which span from 0.2926 to 0.4926. In fuzzy theory, this range can be expressed as $[0.3926]^\alpha = [0.2926 + 0.1\alpha, 0.4926 - 0.1\alpha]$ for $0 \leq \alpha \leq 1$. A similar analysis applies to P_2 , where the parameter τ varies between 0.1661 and 0.3661, represented as $[0.2661]^\alpha = [0.1661 + 0.1\alpha, 0.3661 - 0.1\alpha]$ for $0 \leq \alpha \leq 1$. Consequently, the actual data for both periods P_1 and P_2 falls within the boundaries defined by these upper and lower limits.

This comprehensive analysis has emphasized the capabilities of fuzzy modeling in understanding the dynamics of the COVID-19 pandemic. By applying fuzzy frameworks to both SAIR models with lifelong and non-lifelong immunity, we have not only demonstrated the adaptability and versatility of these models in capturing real-world complexities but also highlighted their capacity to provide accurate predictions. The incorporation of fuzzy parameters, such as τ , has allowed us to better align model outputs with actual data, ultimately enhancing the reliability of our predictions. Additionally, our examination on the upper and lower bounds of the parameter τ within the fuzzy environment has illustrated the sensitivity of the model to this pivotal parameter, underscoring its importance in pandemic modeling.

CONCLUSION

The transmission of infectious diseases occurs in a diverse population. With epidemiological modeling, we can divide the heterogeneous population into subgroups or subpopulations, where each group can have similar characteristics. SIR (Susceptible-Infected-Recovered) type models are compartmental models that can be expanded by incorporating new compartments and new parameters into the

models. In this paper, we consider the SAIR (Susceptible-Asymptomatic-Infected-Recovered) model, where the population is divided into four subgroups; namely susceptible (S), asymptomatic (A), infected (I), and recovered (R). The main idea of considering the infected individuals into two groups, asymptomatic (A) and infected (I), is due to the fact that some individuals do not show any symptoms of the disease but can spread the disease to others, thus categorizing them as asymptomatic individuals. Conversely, individuals who contract the disease and display symptoms can be identified and isolated from the broader society, categorizing them as symptomatic infected individuals.

In this paper, we modified the SAIR model in two distinct ways. The first version includes lifelong immunity, where individuals who recover from the disease are protected from future infections. In contrast, the second version incorporates non-lifelong immunity, allowing individuals who have recovered to potentially become infected again. Both models involve multiple parameters that determine the transition rates between various components. In particular, we emphasize a crucial parameter related to the vaccination of the disease. Here we assume that the vaccinated individuals do not directly move to the recovered state. Significantly, the vaccine effectiveness parameter in these models is addressed from a fuzzy perspective due to its significant role in preventing the spread of the disease.

Our study addresses into the assumption that vaccinated individuals do not directly transition to the recovered state within the SAIR model framework. This assumption is crucial as it acknowledges the possibility of vaccinated individuals contracting the disease despite vaccination. By not immediately moving vaccinated individuals to the recovered state, we capture the temporal gap between vaccination

and the development of immunity. This delay accounts for scenarios where vaccinated individuals may still be susceptible to infection or transmission, thereby providing a more realistic illustration of disease dynamics in the presence of vaccination. This modeling approach enables us to explore the complexities of disease spread, particularly the potential for breakthrough infections among vaccinated individuals, and underscores the importance of vaccination effectiveness in minimizing disease transmission.

From the available data on COVID-19 cases in Turkey, we derive the parameters for the two modified SAIR models. It is important to note that we have access to only two types of real data; infected and recovered cases, as provided by the Ministry of Health. However, our models consist of four compartments. To bridge this gap, we calculate the number of *active cases*, as daily infected cases do not precisely correspond to the active cases used in the SAIR model. This involves creating the active case data set by subtracting the number of deaths and recovered cases from the total infected cases.

Based on the estimated model parameters, it is worth mentioning that the transition rate of the asymptomatic compartment β_A is higher than that of the symptomatic compartment β_I . This observation aligns with the understanding that the virus is predominantly transmitted by asymptomatic individuals from a biological standpoint. Additionally, our model simulations closely match the data for *Active* and *Recovered* cases. Furthermore, the 7-day future predictions are consistent with the data provided by the Ministry of Health in Turkey. This reflects the model's effectiveness in capturing and predicting the dynamics of the COVID-19 pandemic.

Introducing fuzziness into the model has effectively accommodated real data within the range defined by the upper and lower bounds of the simulations. This approach simplifies the management of infected individuals, leading to earlier diagnoses and financial benefits. Working within a fuzzy environment consistently provides valuable new insights and information in disease research. Furthermore, implementing fuzzy models can reduce healthcare costs and allocate resources more efficiently, benefiting healthcare systems and alleviating economic burdens.

ACKNOWLEDGEMENTS

The authors would like to express his sincere thanks to the editors and the anonymous reviewers for their helpful comments and suggestions.

AUTHORSHIP CONTRIBUTIONS

Authors equally contributed to this work.

DATA AVAILABILITY STATEMENT

The authors confirm that the data that supports the findings of this study are available within the article. Raw

data that support the finding of this study are available from the corresponding author, upon reasonable request.

CONFLICT OF INTEREST

The author declared no potential conflicts of interest with respect to the research, authorship, and/or publication of this article.

ETHICS

There are no ethical issues with the publication of this manuscript.

REFERENCES

- [1] Woo PCY, Lau SKP, Huang Y, Yuen K. Coronavirus diversity, phylogeny and interspecies jumping. *Exp Biol Med* 2009;234:1117–1127. [\[CrossRef\]](#)
- [2] Hu B, Ge X, Wang L, Z S. Bat origin of human coronaviruses. *Virology* 2015;12:1–10. [\[CrossRef\]](#)
- [3] Huang C, Wang Y, Li X, Ren L, Zhao J, Hu Y, Zhang L, Fan G, Xu J, Gu X, et al. Clinical features of patients infected with 2019 novel coronavirus in Wuhan, China. *Lancet* 2020;395:497–506. [\[CrossRef\]](#)
- [4] Cucinotta D, Vanelli M. WHO declares COVID-19 a pandemic. *Acta Biomed* 2020;91:157.
- [5] Guan W, Ni Z, Hu Y, Liang W, Ou CQ, He J, et al. Clinical characteristics of coronavirus disease 2019 in China. *N Engl J Med* 2020;382:1708–1720. [\[CrossRef\]](#)
- [6] World Health Organization (WHO). Director-General's remarks at the media briefing on 2019-nCoV on 11 March 2020. (Accessed Mar 11, 2020).
- [7] Daley DJ, Gani J. *Epidemic modelling: An introduction*. Cambridge: Cambridge Univ Press; 2001.
- [8] Chowell G, Hengartner N, Castillo-Chavez C, Fenimore PW, Hyman JM. The basic reproductive number of Ebola and the effects of public health measures: The cases of Congo and Uganda. *J Theor Biol* 2004;229:119–126. [\[CrossRef\]](#)
- [9] Hartley D, Morris JG, Smith DL. Hyperinfectivity: A critical element in the ability of *V. cholerae* to cause epidemics? *PLoS Med* 2005;3:e7. [\[CrossRef\]](#)
- [10] Chowell G, Nishiura H. Transmission dynamics and control of Ebola virus disease EVD: A review. *BMC Med* 2014;12:1–17. [\[CrossRef\]](#)
- [11] Hethcote HW. The mathematics of infectious diseases. *SIAM Rev* 2000;42:599–653. [\[CrossRef\]](#)
- [12] Ortega NRS, Sallum PC, Massad E. Fuzzy dynamical systems in epidemic modelling. *Kybernetes* 2000;29:201–218. [\[CrossRef\]](#)
- [13] Baldemir H, Agah A, Ömer A. Fuzzy modelling of COVID-19 in Turkey and some countries in the world. *Turk J Math Comput Sci* 2020;12:136–150. [\[CrossRef\]](#)

- [14] Abdy M, Side S, Annas S, Nur W, Sanusi W. An SIR epidemic model for COVID-19 spread with fuzzy parameter: The case of Indonesia. *Adv Differ Equ* 2021;2021:1–17. [\[CrossRef\]](#)
- [15] de León UAP, Pérez ÁG, Avila-Vales E. An SEIARD epidemic model for COVID-19 in Mexico: Mathematical analysis and state-level forecast. *Chaos Solitons Fractals* 2020;140:110165. [\[CrossRef\]](#)
- [16] Ahumada M, Ledesma-Araujo A, Gordillo L, Marín JF. Mutation and SARS-CoV-2 strain competition under vaccination in a modified SIR model. *Chaos Solitons Fractals* 2023;166:112964. [\[CrossRef\]](#)
- [17] Anderson RM. Discussion: The Kermack-McKendrick epidemic threshold theorem. *Bull Math Biol* 1991;53:1–32. [\[CrossRef\]](#)
- [18] Liu WM, Hethcote HW, Levin SA. Dynamical behavior of epidemiological models with nonlinear incidence rates. *J Math Biol* 1987;25:359–380. [\[CrossRef\]](#)
- [19] Li MY, Muldowney JS. Global stability for the SEIR model in epidemiology. *Math Biosci* 1995;125:155–164. [\[CrossRef\]](#)
- [20] Ottaviano S, Sensi M, Sottile S. Global stability of SAIRS epidemic models. *Nonlinear Anal Real World Appl* 2022;65:103501. [\[CrossRef\]](#)
- [21] Barbisch D, Koenig KL, Shih FY. Is there a case for quarantine? Perspectives from SARS to Ebola. *Disaster Med Public Health Prep* 2015;9:547–553. [\[CrossRef\]](#)
- [22] Niu Y, Li Z, Meng L, Wang S, Zhao Z, Song T, Lu J, Chen T, Li Q, Zou X. The collaboration between infectious disease modeling and public health decision-making based on the COVID-19. *J Saf Sci Resil* 2021;2:69–76. [\[CrossRef\]](#)
- [23] Liu Z, Magal P, Seydi O, Webb G. Understanding unreported cases in the COVID-19 epidemic outbreak in Wuhan, China, and the importance of major public health interventions. *Biology (Basel)* 2020;9:50. [\[CrossRef\]](#)
- [24] Griette Q, Magal P, Seydi O. Unreported cases for age dependent COVID-19 outbreak in Japan. *Biology (Basel)* 2020;9:132. [\[CrossRef\]](#)
- [25] Tomochi M, Kono M. A mathematical model for COVID-19 pandemic—SIIR model: Effects of asymptomatic individuals. *J Gen Fam Med* 2021;22:5–14. [\[CrossRef\]](#)
- [26] Robinson M, Stilianakis NI. A model for the emergence of drug resistance in the presence of asymptomatic infections. *Math Biosci* 2013;243:163–177. [\[CrossRef\]](#)
- [27] Ministry of Health of Turkey. General coronavirus chart. Available from: <https://covid19.saglik.gov.tr/TR66935/genel-koronavirus-tablosu.html> Accessed Apr 21, 2022.
- [28] Zadeh LA. Fuzzy sets. *Inf Control* 1965;8:338–353. [\[CrossRef\]](#)
- [29] Klir GJ, Yuan B. Fuzzy sets and fuzzy logic: Theory and applications. Upper Saddle River (NJ): Prentice Hall; 1995.
- [30] Akin Ö, Khaniyev T, Oruç Ö, Türkşen I. An algorithm for the solution of second order fuzzy initial value problems. *Expert Syst Appl* 2013;40:953–957. [\[CrossRef\]](#)
- [31] Rezaeifar M, Zare Mehrjerdi M, Nezamabadi-pour H, Mehrabi Boshir Abadi H. Designing a sustainable development model for agricultural sector under critical circumstances (COVID-19 pandemic): A fuzzy approach. *Iran J Fuzzy Syst* 2023;20:173–200.
- [32] Singh M, Pant M, Kong L, Alijani Z, Snášel V. A PCA-based fuzzy tensor evaluation model for multiple-criteria group decision making. *Appl Soft Comput* 2023;132:109753. [\[CrossRef\]](#)
- [33] Khasan A, Rodríguez-López R, Shahidi M. New differentiability concepts for set-valued functions and applications to set differential equations. *Inf Sci* 2021;575:355–378. [\[CrossRef\]](#)
- [34] Yıldırım HB, Kullu K, Amrahov ŞE. A graph model and a three-stage algorithm to aid the physically disabled with navigation. *Univ Access Inf Soc* 2023;1–11. [\[CrossRef\]](#)
- [35] Feoli E. Classification of plant communities and fuzzy diversity of vegetation systems. *Community Ecol* 2018;19:186–198. [\[CrossRef\]](#)
- [36] Mota MTD, Bressane A, Roveda JAF, Roveda SRMM. Classification of successional stages in Atlantic forests: A methodological approach based on a fuzzy expert system. *Cienc Florest* 2019;29:519–530. [\[CrossRef\]](#)
- [37] Rahman MU, Arfan M, Shah K, Gómez-Aguilar J. Investigating a nonlinear dynamical model of COVID-19 disease under fuzzy Caputo, random and ABC fractional order derivative. *Chaos Solitons Fractals* 2020;140:110232. [\[CrossRef\]](#)
- [38] Doğan N, Bayeğ S, Mert R, Akin Ö. Singularly perturbed fuzzy initial value problems. *Expert Syst Appl* 2023:119860. [\[CrossRef\]](#)
- [39] MATLAB. Version 9.9 (R2020b). Natick (MA): The MathWorks Inc; 2020.